MULTIWALL CARBON-NANOTUBE INTERCONNECTS: RADIAL EFFECTS ON PHYSICAL MODELS AND RESISTANCE CALCULATIONS FOR VARIOUS METAL SUBSTRATES

S. Bellucci[1], P. Onorato[1,2], Yuri N. Shunin[3,4], Yuri F. Zhukovskii[4], Natalia Burlutskaya[3]

[1]INFN-Laboratori Nazionali di Frascati, Via E. Fermi 40, 00044 Frascati, Italy
E-mail: bellucci@lnf.infn.it
[2]Department of Physics "A. Volta", University of Pavia, Via Bassi 6, I-27100 Pavia, Italy
[3]Information Systems Management Institute, Riga, Latvia 4 Institute of Solid State Physics, University of Latvia, Riga, Latvia

Abstract–*Based on a model with singular attractive potential of equidistant conductive cylinders, we illustrate an approach to calculate the electron spectrum of metallic multiwall carbon nanotubes (MW CNT) with an arbitrary number of coaxial layers. We compute the number of electrically active channels, N_{ch}, in the ideal case when all MW CNT shells are contacted to the electrodes, starting from the one-electron spectrum. The dependence of N_{ch} on the temperature and on both the innermost and outermost shells radii allows us to discuss the potential performances of MW CNT interconnects, affecting the power dissipation of integrated circuits. Our description improves over the isolated shells model, where band structures remain unaffected from each other. It turns out that, for a small innermost radius MW CNT, when all the shell are contacted to the electrodes, the presence of a geometrical potential can be quite relevant. At the same time, we prove the relevance of the inter-shell in determining N_{ch}, for an outermost shell having hundreds of nanometers radius.*

We then turn our attention to the junctions of carbon nanotubes with contacting metallic elements of a nanocircuit, carrying out numerical simulations on the contacts resistance, using multiple scattering theory and the effective media cluster approach. Calculations for different multiwalled nanotube-metal contacts yield quantitatively realistic results, from several to hundreds kOhm, depending on nanotube chirality, diameter and thickness. As an indicator of possible 'radial current' losses the inter-wall transparency coefficient for MW CNT has been also simulated.

Keywords: *Carbon nanotubes, interconnections, integrated circuits, nanoporous alumina, scattering theory, electronic structure calculations.*

1. INTRODUCTION

Carbon Nanotubes (CNT) are prototype 1-dimensional carbon systems and represent promising candidates for future applications, such as new conductors for nano-electronics [1-3], cold electron sources for field emission [4-8], new materials for nano-mechanics, because they are extremely stiff and resistant to bending [9]. They are basically rolled up sheets of graphene forming tubes that are only nanometers in diameter and have length up to some microns, see Fig. 1.

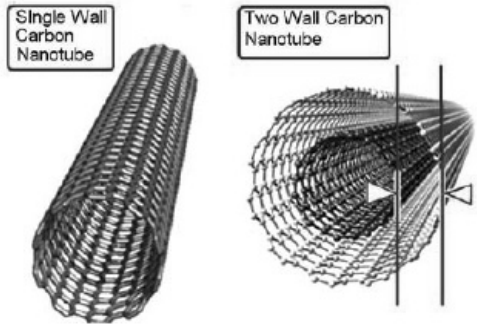

Fig. 1a. SW CNT are basically rolled up sheets of graphite forming tubes that are only nanometers in diameter and have length up to some microns, whereas MW CNT are typically made of several concentrically arranged graphene sheets.

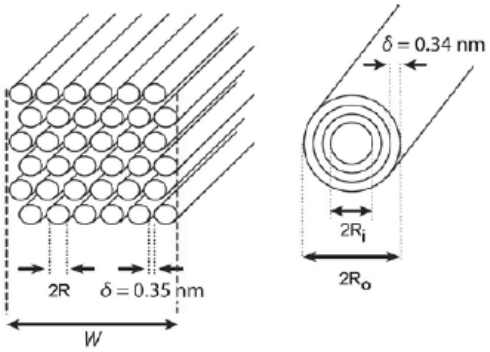

Fig 1b. The inter-shell distance δ is constant and equal to the inter-graphene distance of 0.34 nm, while the number of shells can be evaluated starting from the innermost and the outermost tube radii, R_i and R_o as $(R_o - R_i)/\delta$. MW CNT may have diameters in a wide range of a few to hundreds of nanometers. SW CNT can be thought of, as the fundamental cylindrical structure, forming the building blocks of both MW CNTs and the arrays of SW CNTs, also in bundles.

978-1-4244-5781-6/10/$26.00 © 2010 IEEE

CNT may be grown as single-walled (SW CNT) or multi-walled (MW CNT, typically made of several concentrically arranged graphene sheets). They exhibit semiconducting or metallic properties, depending on the helicity of the carbon rings around the tubule [10-11]. Several techniques have been developed to produce CNTs in sizeable quantities, including arc synthesis and laser ablation (the two early methods to produce SW-CNTs), chemical vapor deposition (CVD) and related techniques [12-14].

The performance and power dissipation of integrated circuits (IC) are largely affected by interconnects. CNTs show great potential in addressing some of the major interconnect challenges in future generations of technology, when copper conductivity will degrade substantially because of size effects. In fact, the copper interconnect is actually used with minimum feature sizes down to 130 nm [15-16]. However many problems are due to the electrical resistivity of copper, which increases with a decrease in dimensions, due to electron surface scattering and grain-boundary scattering [17-18], and to the electromigration failure of copper lines [19-21]. Such size effects arise from interface roughness and small grain size, which are hard to overcome [18]. Thus, in the last decade CNT have been envisioned as a possible replacement for copper electrical interconnects for future gigascale integration [22-27]. Especially, highly aligned parallel CNT architectures comprising all-metallic SW CNT are expected to outperform copper, in terms of failure current density, power dissipation, and on-chip signal transfer delays [28-32]. Since the current carrying capacity of CNTs did not degrade after 350h at current densities of 10^{10}A/cm^2 at 250^{o}C [33] and their thermal conductivity [34, 35] is about 1700-3000W/mK, in recent years CNTs were proposed to develop an innovative cost-effective and reliable technological solution for high-performance next generation nano-interconnects beyond the limitations of the current technology [36]. CNTs interconnects will have high-transmission speed, high current density, exceptional mechanical and thermal properties, optimum signal and power integrity [36].

A central role in determining the electronic properties of a MW CNT as interconnect is played by the number of electrically active channels, N_{ch}. We will discuss a recent calculation of for MW CNTs in the ideal case where all the shells are contacted to the electrodes, by including the effects of the radial terms of the Hamiltonian, usually disregarded [37]. At first, we will show that an intrinsic doping due to the geometrical energy shift can be relevant, when the innermost tube radius becomes of the order of a few nanometers. In fact, when all the shells of a MW CNT are connected to a metallic contact, the Fermi level is shifted and is the same for all internal shells in the CNT. This is equivalent to a doping effect on the CNT.

Then, we shall develop an approach to calculate the electron spectrum of metallic MW CNT with an arbitrary number of coaxial layers by including the inter tube coupling. We demonstrate that the intershell tunneling can be quite relevant in determining N_{ch}, when the radius of the outermost shell becomes of the order of hundreds of nanometers [37]. Our model improves that derived for isolated shells, with band structures unaffected by each other. Starting from our calculation compact physical models can be developed to determine the ultimate potential performances of MW CNT, with various diameters and lengths, and compare them with copper wires and SWNT bundles. Thus, such results offer important guidelines on which kind of CNTs need to be developed, for various interconnect applications.

We then turn our attention to the junctions of carbon nanotubes with contacting metallic elements of a nanocircuit, carrying out numerical simulations on the contacts resistance, using multiple scattering theory and the effective media cluster approach. Calculations for different MW CNT-metal contacts yield quantitatively realistic results, from several to hundreds kΩ, depending on the nanotube chirality, diameter and thickness [38]. As an indicator of possible 'radial current' losses we also report on the simulation of the inter-wall transparency coefficient for MW CNT [38].

2. NUMBER OF CHANNELS AND CNT INTRINSIC RESISTANCE

The electronic properties of a MW CNT as an interconnect strongly depend on the number of electrically active channels, N_{ch}. In fact, even under the hypothesis of ballistic conduction, i.e. when the length of SW CNT is lower than the

mean free path, l_{mfp}, a metallic SW CNT yields an intrinsic resistance R_i of the order of $k\Omega$, accounting for the effect of the voltage drop at the CNT metallic electrode interfaces, $R_i = h/(2 N_{ch} e^2)$, which represents the lowest theoretical and measurable equivalent d.c. resistance of a metallic SW CNT.

Obviously a crucial role in determining the value of N_{ch} is played by the nature of the metallic contacts. Although initially most experiments indicated that only the outer shell in a MW CNT conducts, in recent years it has been shown that all shells can conduct, provided they are properly connected to the contacts [39-43]. Moreover, in general, contacts do not behave in an ideal way. In the case of imperfect contacts, an additional resistance should be added to R_i. In order to achieve low resistances, not only should all shells conduct, but the contact resistance for each shell should also be relatively small. In this case MW CNT may be adopted for large-scale integration. In this section we focus on the calculation of N_{ch} in MW CNT, in the ideal case when all shells are contacted to the electrodes. This is the fundamental physical parameter needed, in order to evaluate the main transport properties of the MW CNT [34-36]. In earlier calculations [34-36] at least two factors were neglected:

I) when the Schroedinger equation for a spinless charged particle constrained to a curved surface is derived using a thin-layer procedure, the latter gives rise to the well-known geometric potential [44-46]. This extra energy can be usually disregarded in SW CNT, whereas it can give relevant effects for MW CNT, when all shells are contacted.

II) In general the one-electron spectrum in MW CNT depends on the presence of the neighboring shells. In fact, the importance of the intertube coupling in MW CNT was proven, in the interpretation of experimental data on electric transport properties of MW CNT [47-48].

In a recent paper [37] we developed a theoretical approach useful to calculate the electron spectrum of metallic MW CNT, with an arbitrary number of coaxial layers. This approach assumes the metallic MW CNT as a set of equidistant coaxial cylinders with attractive Kronig-Penney-type potential along the radius and studies the electron states of such a system. It allows us to calculate the energy level splitting due to the intertube hopping, for MW CNT with any number of coaxial tubes. The bottom subbands energies are shifted by the presence of the geometrical term discussed earlier, [37] according to the plot reported in the top panels of Fig. 2. In Fig. 2 top left the effects due to the geometrical term are reported in the van Hove singularities (bottom of the subbands), for different radius CNT. The geometrical term shifts the bandstructure significantly for small radius CNT, while the contribution becomes negligible for large radius CNT. A schematic representation of the bandstructure for a 7 shells MW CNT is reported in the top right panel, where the effects of the geometrical term are emphasized for each shell.

An intrinsic doping due to the geometrical energy shift can be relevant, when the innermost tube radius becomes of the order of a few nanometers. In fact, when all shells of a MW CNT are connected to a metallic contact, the Fermi level is shifted and is the same for all internal shells in the CNT. This is equivalent to a doping effect on the CNT. Thus, we are able to analyze the effects of the radial term, in determining the number of open channels in a MW CNT.

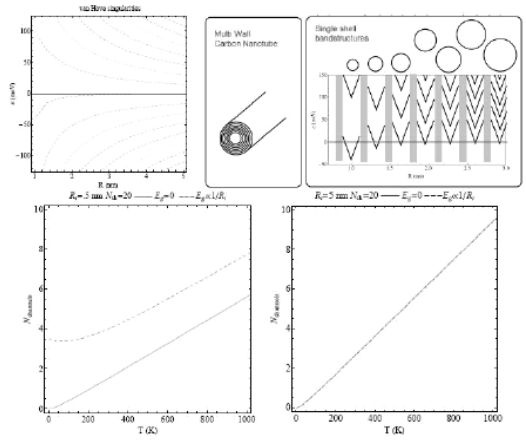

Fig. 2. (Top left) The van Hove singularities (bottom of the subbands) for different radius CNT. The geometrical term shifts the bandstructure significantly for small radius CNT, while the contribution becomes negligible for large radius CNT. (Top Right) Schematic representation of the bandstructure for a 7 shell MW CNT. We report both the shell circumferences and the corresponding bandstructure. (Bottom) The calculated number of conducting channels for a MW CNT with 20 shells and different inner radius versus temperature. The Fermi energy (the chemical potential of the contacts) is supposed to be fixed to the Fermi level of the innermost tube. It follows that the N_{ch} vs T behaviour deviates from the ideal linear case, when the innnermost tube is thin (left panel with R_i =0.5nm), while the continuum approximation plays well, when the innermost radius is above a few nanometers (right panel with R_i =5nm).

In the bottom panels of Fig. 2 the calculated numbers of conducting channels as a function of temperature are reported, [37] for a MW CNT with 20 shells and different inner radius. The Fermi energy (i.e. the chemical potential of the contacts) is supposed to be fixed to the Fermi level of the innermost tube. It follows that the N_{ch} vs T behaviour deviates from the ideal linear case, when the innermost tube is thin, while the continuum approximation plays well, when the innermost radius is above a few nanometers.

Thus, following the approach reported earlier, [37] we are able to evaluate the number of electrically active channels, N_{ch}. In Fig. 3 we report the number of conduction channels, for different geometries of MW CNT calculated at T = 300K. These CNT differs both for the inner radii (from 10 to 200 nm) and for the number of shells (from 5 to 50).

The results reported show that the effects of the intershell hopping cannot be disregarded, when the radius (and/or the number of shell) becomes too large. The main effect of the increased number of channels, and the quadratic corrections to the dependence of *Nch* on R are clearly shown in the left and right panels of Fig. 3 respectively.

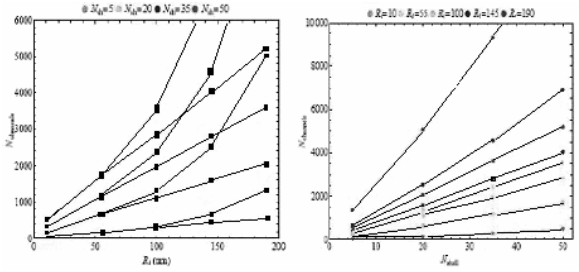

Fig. 3. Number of conduction channels for different geometries of the MW CNT, calculated at T = 300K. The CNT differ both for the inner radii (from 10 to 200 nm) and for the number of shells (from 5 to 50). The dashed line are obtained neglecting the intershell coupling. On the left, a quadratic deviation from this behaviour is clearly shown.

3. CNT-METAL JUNCTION RESISTANCE RESULTS

Next, we illustrate of our study with simulations of conductivity and resistivity, carried out using the multiple scattering theory and the effective media cluster approach. The main problems at the current stage of researches on CNT interconnect resistance appear due to the influence of chirality effects in interconnects of SW and MW CNT with the fitting metals (Me = Ni, Cu, Ag, Pd, Pt, Au) for predefined CNT geometry. The main task of this section is the implementation of advanced ab initio simulation models for the construction of nanocircuits containing CNTs and their junctions with metallic contacts. Both the local and integral CNT properties have been simulated using prototype CNT models such as a dispersion law, the electronic density of states (EDOS), the conductivity, resistivity, effective masses, etc.

The scattering theory approach allows us to calculate both the electronic structure and elastic properties of condensed matter considered as the static phenomena simultaneously with the dynamical phenomena of the electron transport. A computational procedure developed for these calculations [49] is based on construction of the cluster potentials and evaluation of the S-and T-matrices for scattering and transfer, respectively. Certain approximations are necessary to obtain reliable results. For instance, the CPA (coherent-potential approach [50]) is considered as an effective-medium-approximation (EMA). The specific conductivity (σ) could be evaluated through the Kubo-Greenwood formalism [49, 50] or, in simple cases, using the Drude-type formula. The specific resistivity (ρ) could be described through participations of charge carriers in transport according to various mechanisms based on the scattering centers, namely, atoms of clusters, phonons, charge defects, structural defects, etc., including the pure elastic way, called as ballistic. The temperature and frequency properties can be also described and estimated using the formalism of scattering theory.

The first step in the CPA-EMA modeling is the construction of potentials, both atomic and crystalline which uses the special well-tested analytical procedures based the Gaspar-like potentials and $X_{\acute{a}}$ and $X_{\acute{a}\hat{a}}$ presentations for the electronic exchange and correlation in form of the electronic density expansions [49]. Then, to obtain the electronic structure, the calculations on scattering properties are necessary, generally, in the form of S- and T-matrices. The electronic structure calculations begin with the definition of the initial atomic structure to produce a medium for solution of the scattering problem for a trial electronic wave [49]. As the zero approach in the modeling procedure, one postulates the atomic structure on the level of short- and medium-range orders. Further calculations on the density

of the corresponding electronic states (DOS) can be done using the variation principles.

There exist a few algorithms both to estimate the conductivity in static and frequency regimes as well as to take into account the temperature effects. However, in the case of CNT we must consider not only the diffusive mechanism of conductivity, but also the 'so-called' ballistic one. This is an evident complication for the interpretation of electrical properties of CNT and their systems.

The CPA-EMA model of the CNT-Ni nanointerconnect [51] is developed in a recent paper [38]. Within the formalism of electronic transport it consists of two regions supporting two different electron transport mechanisms: ballistic (elastic) and collisional (non-elastic).

a) The mechanism of ballistic conductivity, as a result of multiple scattering (valid for CNT and metal substrate). We assume that the conducting nanotubes are not so long and the electrons are not scattered too much by any defect (imperfection) of this nanomaterial. The effect of the charge accumulation is neglected here as well. This situation is similar to an ideal billiard with moving elastic balls-electrons, according to the Landauer model [52].

(b) Non-elastic mechanism. Using the simulation models, presented earlier, [49, 51] we consider a resistance model for the metal interconnect with single- and multi-wall (SW and MW) CNTs based on evaluation of the interface potential barriers and implementation of Landauer's formula. All resistance calculations have been performed taking into account that not all the electrons participate in a conduction process with the Fermi velocity. For this aim, we must take into account the thermally activated electrons. The reason for determination of thermally activated electrons is caused by the scattering mechanism, which is changing in the space of CNT-Metal interconnect.

I. SW CNT simulations The 'effective bonds' model means that the conductivity of CNT-metal interconnect is proportional to the number of direct chemical bonds between CNT and metal, which depend on the CNT chirality and metal substrate atomic configuration. Thus, we can evaluate the Landauer's multiplier for conductance calculations. We have also proposed a parameter φ (chirality angle) for the identification of nanotube chirality. Our results show the effect of the nanotube diameter and chirality on CNT-Ni interconnect resistivity. It is clear that the larger is the CNT diameter, the larger the number of direct junction bonds and the total conductance (i.e., the resistance is smaller). A similar effect is observed for varying chirality: the number of direct bonds is higher for armchair and zigzag CNT chiralities. We also compared the resistance for the interconnects of the same SW CNT with various metal substrates (Ag, Au, Cu, Ni, Pd and Pt). Although nickel is a good catalyst for CNT growth, resistance of its interconnect with nanotube has been found to be noticeably higher as compared to that for silver, gold and platinum substrates.

II. MW CNT simulations Using the simulation models presented earlier [49, 51] we have developed a model of multi-wall CNT-Me junction resistance based on the interface potential barriers evaluation and Landauer's formalism described above. Using the Landauer's formula for the conductivity, we have estimated the effective resistance of MW CNT-Me junctions, taking into account only thermally activated electrons. Our calculations allow for a comparison of resistance values of junctions between the considered MW CNT and the same metal substrates as presented above in the case of SW CNTs. We can conclude that for the interconnects of metals with both SW and MW CNTs, the smaller resistance is again observed for Ag, Au and Pt. Obviously, resistance of the metal interconnect with MW CNT is several times smaller than that with SW CNT since the number of direct junction bonds is substantially larger in the former case.

III. Evaluation of current losses between the adjacent shells in MW CNT Using the model of interwall potential in MW CNT we also evaluate the coefficient of transparency which determines the possible 'radial current' losses. Transparency T per one C-C bond along the interwall distance determines the radial current losses. For example, if the larger shell possesses the zigzag chirality whereas chirality of the smaller one is armchair while distance between them is a = 13.54-12.88 = 0.66 nm, the radial current loss factor can be estimated as $T = 3.469\ 10^{-6}$ per one C-C bond. Using the model of 'effective bonds' developed in current study in the framework of CPA-EMA formalism based on scattering theory and Landauer's approach, we can predict the resistivity properties for both

SW and MW CNT-Me interconnects. Resistance of the latter for the same external nanotube diameter and metal substrate is substantially smaller, i.e., the effectiveness of the multiwall nanotubes for the CNT interconnects is noticeably higher. We have also developed the model of interwall interaction in MW CNT as well as estimated the transparency coefficient as indicator of possible 'radial current' losses.

Acknowledgements–This work was supported in part by the EU under the 7th Framework Program ICT-2007.8.1 FET Proactive 1: Nano-scale ICT devices and systems Carbon nanotube technology for high-speed next-generation nano-Interconnects (CATHERINE) project, Grant Agreement n. 216215.

References

[1] M.S. Dresselhaus, G. Dresselhaus, P. Avouris, Eds. Carbon Nanotubes: *Synthesis, Structure, Properties, and Applications*; Springer-Verlag: pp 256, Berlin, 2001.

[2] S. Bellucci, "Carbon nanotubes: physics and applications". *Phys. Stat. Sol. (c)*, **2**(1), pp. 34–47; 2005.

[3] G. Philip Collins, Phaedon Avouris (December 2000). "Nanotubes for Electronics". *Scientific American*: **67**; S. Iijima, *Nature*, 1991, **354**, pp. 56–58.

[4] J.M. Bonard, H. Kind, T. Stockly and L. Nilsson, *Solid-State Electron*, **45**, 893–914, 2001.

[5] J.M. Bonard, J. P. Salvetat, T. Stockli, L. Forro and A. Chatelain, *Appl. Phys. A*, **69**, pp. 245–254, 1999.

[6] J.M. Bonard, K. A. Dean, B. F. Coll and C. Klinke, *Phys. Rev. Lett.*, **89**, 197602, 2002.

[7] S. Bellucci, C. Balasubramanian, F. Micciulla, A. Tiberia, *J. Phys. Condens. Matter*, **19**, pp. 395014 2007.

[8] S. Bellucci, A. Tiberia, G. Di Paolo, F. Micciulla, C. T. Balasubramanian, *Journal of Nanophotonics*, **4**, 043501, 2010.

[9] M.R. Falvo, G. J. Clary, R. M. Taylor, V. Chi, F. P. Brooks, S. Washburn and R. Superfine, *Nature*, **389**, pp. 582–584, 1997.

[10] N. Hamada, S. I. Sawada, A. Oshiyama, *Phys. Rev. Lett.* **68**, p. 1579, 1992.

[11] R. Saito, *et al.*, *Appl. Phys. Lett.* **60**, p. 2204, 1992.

[12] A.P. Moravsky, E. M. Wexler, R.O. Loutfy , in *Carbon Nanotubes Science and Applications*, ed. M. Meyyappan, CRC Press, Boca Raton, 1th edn., ch. 3, pp. 65–94, 2005.

[13] M. Meyyappan, in *Carbon Nanotubes Science and Applications*, ed. M. Meyyappan, CRC Press, Boca Raton, 1th edn., ch. 4, pp. 99–112, 2005.

[14] S. Bellucci, *Nucl. Instrum. Methods B*, **234**, pp. 57–77, 2005.

[15] S. Yokogawa, N. Okada, Y. Kakuhara, H. Takizawa, *Microelectron. Reliab.* **41**, p 1409, 2001.

[16] X.W. Lin, D. Pramanik, *Solid State Technol.* **41**, p. 63, 1998.

[17] G. Steinlesberger, M. Engelhardt, G. Schindler, W. Steinhogl, A. von Glasow, K. Mosig, and E. Bertagnolli, *Microelectron. Eng.* **64**, p. 409, 2002.

[18] T.S. Kuan, C.K. Inoki, G.S. Ohrlein, K. Rose, Y.P. Zhao, G.C. Wang, S.M. Rossnagel, C. Cabral, *Mater. Res. Soc. Symp. Proc.* **612**, D.7.1.1, 2000.

[19] N.L. Michael, C.U. Kim, P. Gillespie, R. Augur, Electromigration Failure in Ultrafine Copper Interconnects, *J. Electron. Mater.*, **32**, p. 988993, 2003.

[20] International Technology Roadmap for Semiconductors 2007 Edition: Executive Summary, p. 42, http://www.itrs,net/Links/2007ITRS/ExecSum2007.pdf.

[21] Q. Huang, C.M. Lilley, R. Divan, "An In Situ Investigation of Electromigration in Cu Nanowires", *Nanotechnology,* **20**, p. 75706, 2009.

[22] B.Q. Wei, R. Vajtai, P.M. Ajayan, "Reliability and Current Carrying Capacity of Carbon Nanotubes", *Appl. Phys. Lett.*, **79**, p. 1172, 2001.

[23] A. Naeemi, J.D. Meindl, "Monolayer Metallic Nanotube Interconnects: Promising Candidates for Short Local Interconnects", *IEEE Electron Devices Lett.* **26**, p. 544546, 2005.

[24] Y. Homma, T. Yamashita, Y. Kobayashi, T. Ogino, "Interconnection of Nanostructures Using Carbon Nanotubes", *Physica B: Phys. Condens. Matter*, **323**, p. 122123, 2002.

[25] J. Li, Q. Ye, A.Cassell, H.T. Ng, R. Stevens, J. Han, M. Meyyappan, "Bottom-Up Approach for Carbon Nanotube Interconnects", *Appl. Phys. Lett.*, **82**, p. 2491, 2003.

[26] A. Nieuwoudt, Y. Massoud, "Evaluating the Impact of Resistance in Carbon Nanotube Bundles for VLSI Interconnect Using Diameter-Dependent Modeling Techniques", *IEEE Trans. Electron Devices,* **53**, p. 24602466, 2006.

[27] V. Zhirnov, D. Herr, and M. Meyyappan, *J. Nanopart. Res.* **1**, p. 151, 1999.

[28] F. Kreupl, A.P. Graham, G.S. Duesberg, W. Steinho gl, M. Liebau, E. Unger, W. Hoenlein, „Carbon Nanotubes in 8 Interconnect Applications", *Microelectron. Eng.*, **64**, p. 399408, 2002.

[29] K.H. Koo, H. Cho, P. Kapur, K.C. Saraswat, "Performance Comparisons between Carbon Nanotubes, Optical, and Cu for Future High-Performance On-Chip Interconnect Applications", *IEEE Trans. Electron Devices*, **54**, p. 32063215, 2007.

[30] A. Naeemi, J.D. Meindl, "Design and Performance Modeling for Single-Walled Carbon Nanotubes as Local, Semiglobal, and Global Interconnects in Gigascale Integrated Systems", *IEEE Trans. Electron Devices*, **54**, p. 2637, 2007.

[31] A. Naeemi, J.D. Meindl, Compact physical models for multiwall carbon nanotube interconnects, *IEEE Electron Device Letters,* **27**, p. 5, 2006.

[32] Y.C.Chen, N.R. Raravikar, L.S. Schadler, P.M. Ajayan, Y.P. Zhao, T.M. Lu, G.C. Wang, X.C. Zhang, "Ultrafast Optical Switching Properties of Single-Wall Carbon Nanotube Polymer Composites at 1.55", *Appl. Phys. Lett.* **81**, p. 975, 2002.

[33] B.Q. Wei, R. Vajtai, and P. M. Ajayan, *Appl. Phys. Lett.* **79**, p. 1172, 2001.

[34] M.A. Osman and D. Srivastava, *Nanotechnology* **12**, p. 21, 2001.
[35] J. Hone, M. Whitney, C. Piskoti, and A. Zettl, *Phys. Rev. B* **59**, p. R2514, 1999.
[36] A. Naeemi, J.D. Meindl, *Annual Review of Materials Research,* **39**, pp. 255–275, 2009.
[37] S. Bellucci, P. Onorato, "Radial effects on physical Models for Multiwall Carbon-Nanotube Interconnects", submitted for publication (2010).
[38] Y.N. Shunin, Y.F. Zhukovskii, N. Burlutskaya, S. Bellucci, "Resistance simulations for junctions of sw and mw carbon nanotubes with various metal substrates", submitted to *Central European Journal of Physics*, 2010.
[39] M. Nihei, D. Kondo, A. Kawabata, S. Sato, H. Shioya, *et al*., "Low-resistance multi-walled carbon nanotube vias with parallel channel conduction of inner shells", *Proc. IEEE Int. Interconnect Tech. Conf.,* pp. 23436. Piscataway: IEEE, 2005.
[40] Li HJ, Lu WG, Li JJ, Bai XD, Gu CZ, Multichannel ballistic transport in multiwall carbon nanotubes. *Phys. Rev. Lett.* **95**, p. 0866014, 2005.
[41] J.Y. Huang, S. Chen, S.H. Jo, Z. Wang, D.X. Han, e*t al.*, "Atomic-scale imaging of wall-by-wall breakdown and concurrent transport measurements in multiwall carbon nanotubes", *Phys. Rev. Lett.* **94**, p. 2368024, 2005.
[42] I. Takesue, J. Haruyama, N. Kobayashi, S. Chiashi, S. Maruyama, T. Sugai, and H. Shinohara, *Phys. Rev. Lett.* **96**, p. 057001, 2006.
[43] S. Bellucci, M. Cini, P. Onorato and E. Perfetto, *Phys. Rev. B* **75**, p. 014523, 2007.
[44] G. Ferrari, A. Bertoni, G. Goldoni, and E. Molinari *Phys. Rev. B* **78**, p. 115326, 2008.
[45] G. Ferrari and G. Cuoghi, *Phys. Rev. Lett.* **100**, p. 230403, 2008.
[46] A.A. Abrikosov Jr., D.V. Livanov, and A.A. Varlamov *Phys. Rev. B* **71**, pp. 165423, 2005.
[47] S. Frank, P. Poncharal, Z.L. Wang, and W.A. de Heer, *Science* **280**, p. 2829, 2000.
[48] S. Sanvito, Y.-K. Kwon, D. Tomanek, and C.J. Lambert, *Phys. Rev. Lett.* **84**, p. 1974, 2000.
[49] Yu.N. Shunin, K.K. Schwartz. In: *Computer Modelling of Electronic and Atomic Processes in Solids* (Eds. R.C. Tennyson, A.E. Kiv; Kluwer Academic Publisher, Dodrecht, Boston, London, 1997) pp. 241–257.
[50] E.L. Economou. "Green's Functions in Quantum Physics", 3rd Ed., *Solid State Ser.* **7**, Springer Verlag, Berlin, Heidelberg, 2006.
[51] Yu.N. Shunin, Yu.F. Zhukovskii, S. Bellucci, *Computer Modelling and New Technologies* **12**(2), p. 66, 2008.
[52] D. Stone, A. Szafer, *IBM Journal of Research and Development* **32**, p. 384, 1988.